Determination of Material Model of Hyperelastic Material

P. Palička[1,*], R. Huňady[1], P. Lengvarský[1]

[1] *Department of Applied Mechanics and Mechanical Engineering, Faculty of Mechanical Engineering, Technical University of Košice, Letná 9/B, 042 00 Košice, Slovak Republic*

[*] *peter.palicka@tuke.sk*

Abstract: Hyperelastic materials are characterized by the fact that they do not have a linear region in the stress-strain diagram, where there is a linear relationship between stress and strain. Thus, their response on mechanical loading cannot be described by material constants such as Young's modulus and Poisson's ratio. For that purpose strain energy potential is usually used. The paper deals with the evaluation of the material model of hyperelastic material in the Abaqus/CAE using the material data obtained from experimental measurements. The tested samples were made from a vehicle water channel seal. This material can be referred to as closed cell sponge rubber. It is a porous material made of expanded rubber with an air-filled matrix structure. For the purposes of evaluating the material model, tensile tests were performed at two different loading speeds, where digital image correlation system was used to measure deformation. Marlow, Ogden and reduced polynomial forms of strain energy potential were used to fit the hyperelastic material model on the test data.

Keywords: hyperelasticity; hyperelastic material model; tensile test; sponge rubber; DIC.

1 Introduction

Isotropic, linear elasticity theory is characterized by two important physical constants: Young's modulus and Poisson's ratio. In isotropic, nonlinear elasticity theory, the traditional material constants play a less important role because the material response to mechanical loading is not generally described by constants [1]. Hyperelastic materials are often used in engineering practice for the production of tires, seals, washers, mechanical energy absorbers, etc. Hyperelasticity is a property of elastomers that can extend by hundreds of percent of their original length. The mechanical response of hyperelastic materials is sensitive to variety of factors including strain rate, stress state, temperature, etc. Due to the unique cellular structures in foam materials, the Poisson's ratio has been observed to be positive, zero, or even negative, depending on cellular structures, densities, or matrix material. When the foam materials are subjected to large deformations, the material response becomes nonlinear, usually in the form of a plateau followed by a drastic hardening behavior after densification. Such a nonlinear response results in the Poisson's ratio no longer being a constant, but rather varying with strain [2].

Hyperelastic materials are described in terms of a "strain energy potential $U(\varepsilon)$" that defines the strain energy stored in the material per unit of reference volume (volume in the initial configuration) as a function of the strain at that point in the material. There are several forms of strain energy potentials available in Abaqus/CAE to model approximately incompressible isotropic elastomers. In this paper the Marlow, Ogden and the Reduced polynomial are described. Generally, when data from multiple experimental tests are available (typically, this requires at least uniaxial and equibiaxial test data), the Ogden form is more accurate in fitting experimental results. If limited test data are available for calibration, Reduced polynomial form provide reasonable behavior. When only one set of test data (uniaxial, equibiaxial, or planar test data) is available, the Marlow form is recommended. In this case a strain energy potential is constructed that will reproduce the test data exactly and that will have reasonable behavior in other deformation modes [3].

2 Hyperelastic material models

Marlow form

The form of the Marlow strain energy potential is

$$U = U_{dev}(\overline{I}_1) + U_{vol}(J_{el}), \tag{1}$$

where U is the strain energy per unit of reference volume, with U_{dev} as its deviatoric part and U_{vol} as its volumetric part; $\overline{I}_1 = \overline{\lambda}_1^2 + \overline{\lambda}_2^2 + \overline{\lambda}_3^2$ is the first deviatoric strain invariant, where the deviatoric stretches $\overline{\lambda}_i = J^{-\frac{1}{3}}\lambda_i$, J is the total volume ratio, J_{el} is the elastic volume ratio and λ_i are the principal stretches. The deviatoric part of the potential is defined by providing either uniaxial, equibiaxial, or planar test data; while the volumetric part is defined by providing the volumetric test data, defining the Poisson's ratio, or specifying the lateral strains together with the uniaxial, equibiaxial, or planar test data [3].

Ogden form

The form of the Ogden strain energy potential is

$$U = \sum_{i=1}^{N} \frac{2\mu_i}{a_i^2}(\overline{\lambda}_1^{a_i} + \overline{\lambda}_2^{a_i} + \overline{\lambda}_3^{a_i} - 3) + \sum_{i=1}^{N} \frac{1}{D_i}(J^{el} - 1)^{2i}, \tag{2}$$

where N is a material parameter; and μ_i, a_i and D_i are temperature-dependent material parameters. The initial shear modulus and bulk modulus for the Ogden form are given by $\mu_0 = \sum_{i=1}^{N} \mu_i$, $K_0 = \frac{2}{D_1}$ [3].

Reduced polynomial form

The form of the reduced polynomial strain energy potential is

$$U = \sum C_{i0}(\overline{I}_1 - 3)^i + \sum \frac{1}{D_i}(J^{el} - 1)^{2i}, \tag{3}$$

where C_{i0} and D_i are temperature-dependent material parameters. The initial shear modulus and bulk modulus are given by $\mu_0 = 2C_{10}$, $K_0 = \frac{2}{D_1}$ [3].

Hyperelastic material stability

It is common for the hyperelastic material model determined from the test data to be unstable at certain strain magnitudes. Abaqus performs a stability check to determine the strain magnitudes where unstable behavior will occur. Once the strain energy potential is determined, the behavior of the hyperelastic model in Abaqus is established. However, the quality of this behavior must be assessed: the prediction of material behavior under different deformation modes must be compared against the experimental data. An important consideration in judging the quality of the fit to experimental data is the concept of material or Drucker stability. The Drucker stability condition for an incompressible material requires that the change in the stress, $d\sigma$, following from any infinitesimal change in the logarithmic strain, $d\varepsilon$, satisfies the inequality

$$d\sigma : d\varepsilon > 0. \tag{4}$$

Using

$$d\sigma = D : d\varepsilon, \tag{5}$$

where D is the tangent material stiffness, the inequality becomes

$$d\varepsilon : D : d\varepsilon > 0, \tag{6}$$

thus requiring the tangential material stiffness to be positive-definite [3].

3 Experimental measurements

The sample dimensions and tensile test methodology were performed according to STN ISO 37 [4]. The samples were made from a vehicle water channel seal, from the upper part that can be referred to as closed cell sponge rubber (Fig. 1). It is a porous material made of expanded rubber with an air-filled matrix structure.

Tensile tests were performed on a FPZ 100/1 testing machine. Digital image correlation system Q-450 with one high-speed camera was used to measure deformation of the samples (Fig. 2a). Digital image correlation (DIC) is an optical method that allows to measure displacements and surface strains of an object [5]. Deformation fields are determined by correlation of corresponding sub-images called facets before and after loading. Each pattern must contain a characteristic part of the contrast stochastic speckle pattern that needs to be applied on the surface of the sample.

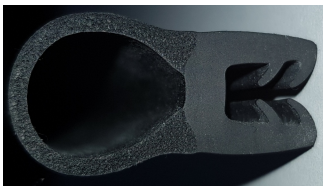

Fig. 1: Rubber seal.

In this work, the pattern was created by dotting with a white marker. This method proved to be the most suitable for creating a pattern on the surface of the rubber sample. The use of pre-printed adhesive vinyl foil was not an option due to its relatively high stiffness and the threat of peeling under large deformations. Creating a pattern using white spray paint also proved inappropriate. The paint had a tendency to fall off after drying. The pattern formed using white marker was stable until the sample was torn. The size of the speckles was optimal with respect to the dimensions of the sample (Fig. 2c). The resulting pattern ensured good image correlation. The deformation field remained compact until the last step, as shown in Fig. 3a. The obtained surface contour of the sample is given by a virtual grid of points. The size of the facets was set to 9 px and the grid size to 5 px. Tensile tests were performed at two speeds 84 mm/min and 600 mm/min. The sampling frequency of the camera was set to 50 fps in the first case and 100 fps in the second case.

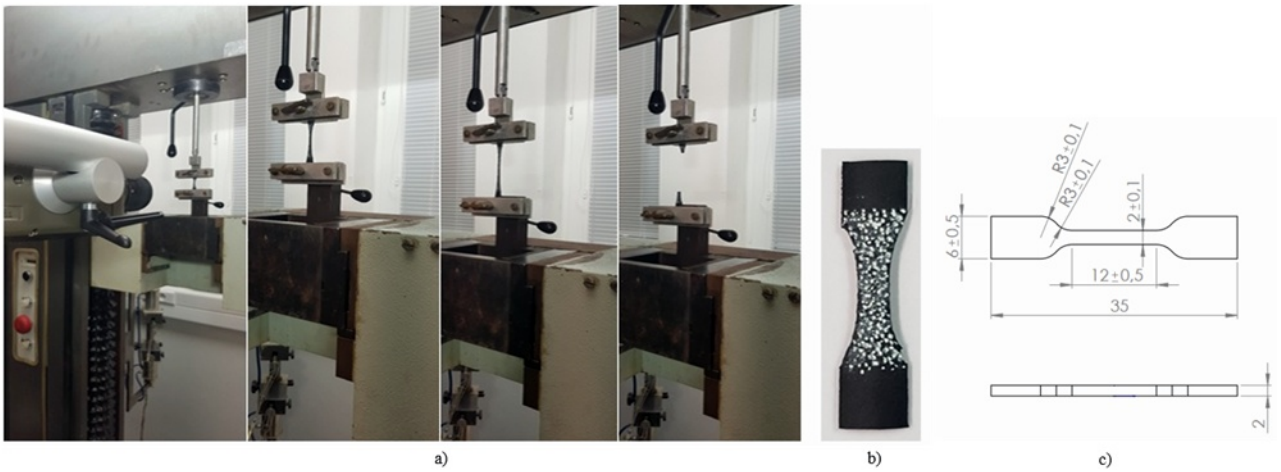

Fig. 2: a) Tensile test; b) Sample with stochastic pattern; c) Sample dimensions.

The tensile force was synchronously measured using a force sensor integrated into the testing machine. The measurements were evaluated in Istra 4D software (Fig. 3a). Nominal stress and nominal strain were calculated according to the procedure defined in the standard [4]. For that purpose, the virtual line gauges were used (Fig. 3b). The nominal strain was determined based on the relative distance of these gauges.

From strain field (see Fig. 3a), the values needed to determine the Poisson ratio were obtained. The Poisson's ratio μ determines the ratio of relative transverse shortening to its relative elongation, i.e.

$$\mu = \frac{-\varepsilon_x}{\varepsilon_y}, \tag{7}$$

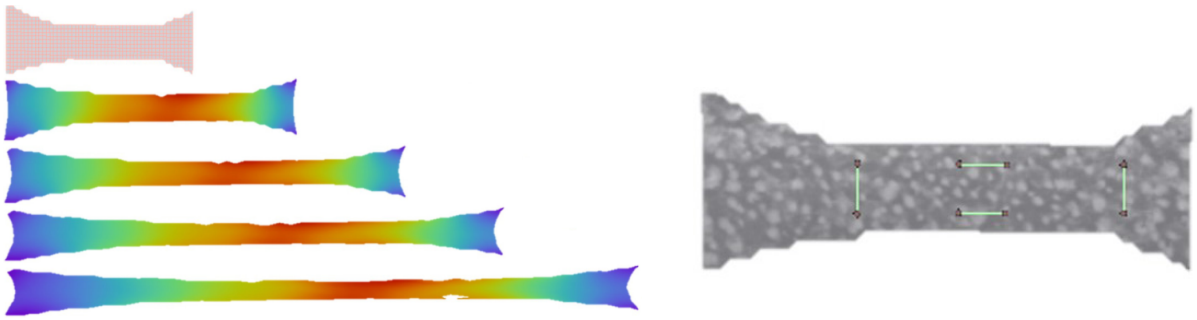

Fig. 3: a) Longitudinal strain field; b) Virtual gauges.

where ε_x and ε_y represent strain in transverse and axial direction, respectively. Their values were obtained from Istra 4D using a virtual line gauges (see Fig. 3b).

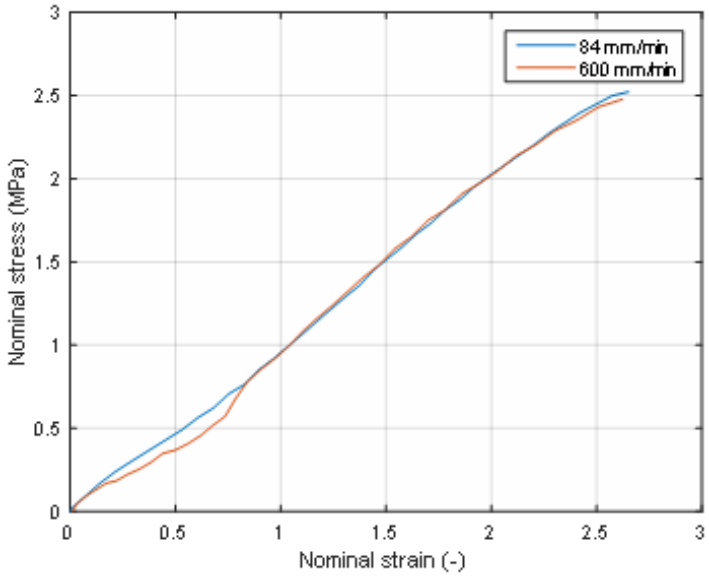

Fig. 4: Stress-strain diagram of tested rubber sponge samples.

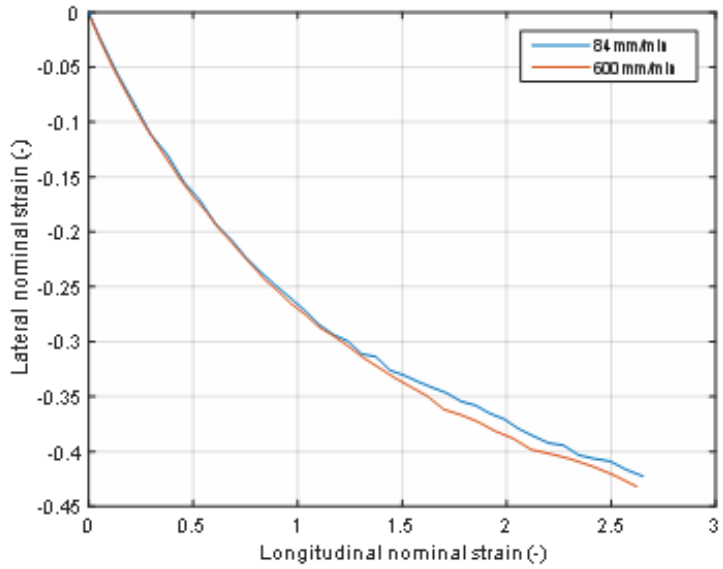

Fig. 5: Lateral vs longitudinal strain of tested rubber sponge samples.

The results of the measurements are shown in the following figures. Fig. 4 shows the stress-strain curve of tested rubber sponge samples for two different loading speed. The dependence of the lateral nominal strain

on the elongation is shown in Fig. 5. Since the strains were evaluated in two perpendicular directions, it was possible to show how the Poisson's ratio decreases with strain (see Fig. 6).

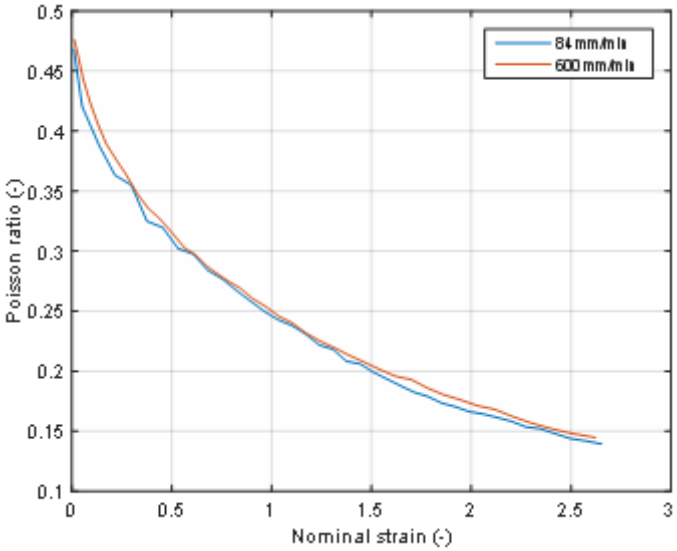

Fig. 6: Poisson's ratio vs longitudinal strain of tested rubber sponge samples.

4 Calibrating a material model

The meausred material data were imported into the Abaqus/CAE to calibrate the hyperelastic material using the "Evaluate" function. This feature allows to predict the behavior of a material model. Calibration process is based on fitting the hyperelastic model to experiment test data. The best fit model must meet two criteria: stability and the least possible fitting errors. Fig. 7 and Fig. 8 show the material characteristics obtained by the fitting process. In addition to the Marlow form, Ogden and Reduced polynomial forms of the higher order were used. The fulfillment of the criteria is given in Tab. 1 and Tab. 2.

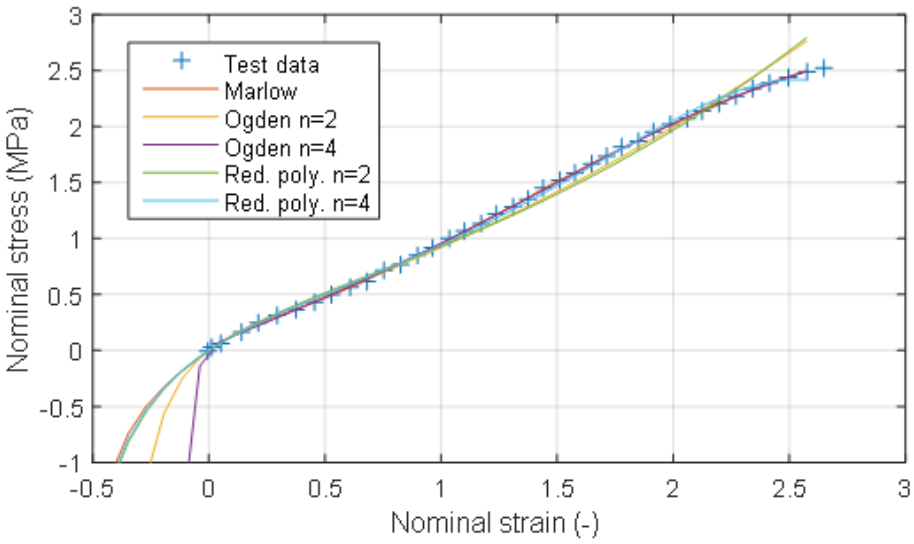

Fig. 7: Fitted stress-strain curves of the sample loaded at a speed of 84 mm/min.

Based on the evaluation of the calibration results of the material models, it was concluded that the Marlow, Ogden 2nd order and Reduced Polynomial 2nd order models are the most suitable with respect to stability for specimens loaded at 84 mm/min and Marlow and Reduced Polynomial 3rd order models for specimens loaded at 600 mm/min. The coefficients of the selected models are given in Table 3.

Tab. 1: Stability and fitting error of the material model at a tensile speed of 84 mm/min.

Stability	Forms				
	Marlow	Ogden n=2	Ogden n=4	Reduced polynom. n=2	Reduced polynom. n=4
Uniaxial tension	Stable	Stable	Stable	Stable	$<$ 2.6800
Uniaxial compression	Stable	Stable	$>$ -0.0930	Stable	$>$ -0.8565
Planar tension	Stable	Stable	$<$ 0.0900	Stable	$<$ 2.600
Planar compression	Stable	Stable	$>$ -0.0826	Stable	$>$ -0.7222
Volumetric tension	Stable	Stable	Stable	Stable	Stable
Volumetric compression	Stable	Stable	Stable	Stable	Stable
Fitting error	-	0.21	0.05	0.31	0.24

Tab. 2: Stability and fitting error of the material model at a tensile speed of 600 mm/min.

Stability	Forms				
	Marlow	Ogden n=2	Ogden n=3	Reduced polynom. n=2	Reduced polynom. n=4
Uniaxial tension	Stable	$<$ 1.7100	$<$ 2.6000	Stable	$<$ 2.7800
Uniaxial compression	Stable	Stable	$>$ -0.9228	Stable	$>$ -0.8628
Planar tension	Stable	Stable	$<$ 2.6000	Stable	$<$ 2.6900
Planar compression	Stable	Stable	$>$ -0.7222	Stable	$>$ -0.7290
Volumetric tension	Stable	Stable	Stable	Stable	Stable
Volumetric compression	Stable	Stable	Stable	Stable	Stable
Fitting error	-	8.99	10.20	13.10	10.18

Tab. 3: Coefficients of Reduced polynomial 2nd order forms.

84 mm/min		600 mm/min
Ogden n=2	Reduced polynomial n=2	Reduced polynomial n=3
μ_1 = 0.32738	C_{10} = 0.2374	C_{10} = -2.4761 $\times$ 10^{-4}
μ_2 = 0.2856	C_{20} = -4.8579 $\times$ 10^{-4}	C_{20} = 0.11091
α_1 = 1.8600		C_{30} = -5.5865 $\times$ 10^{-3}
α_2 = -3.9997		
The other coefficients are zero.		

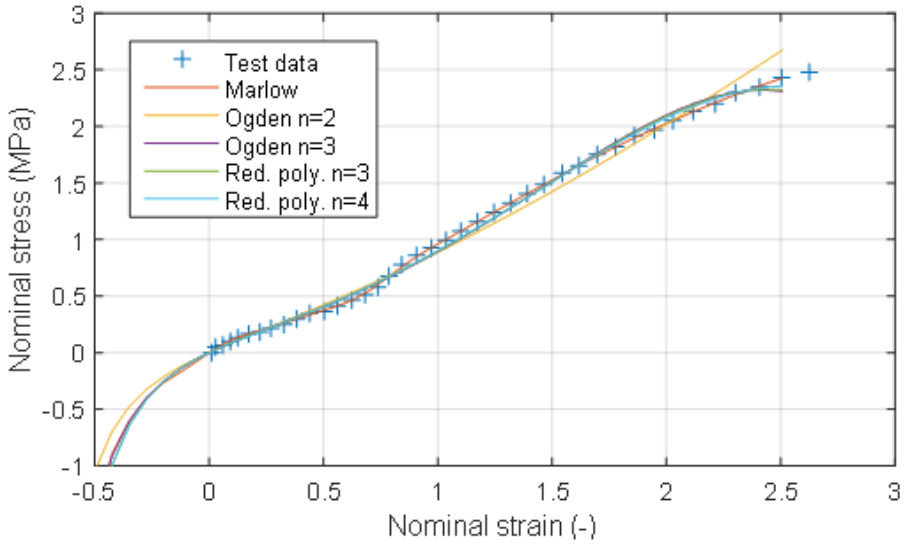

Fig. 8: Fitted stress-strain curves of the sample loaded at a speed of 600 mm/min.

5 Conclusion

The paper presented the process of calibration of hyperelastic material model in the Abaqus/CAE program based on data obtained during tensile tests performed at two load rates. Analyzed material was a porous expanded rubber with an air-filled matrix structure. Marlow, Ogden and Reduced Polynomial forms were used in the fitting process. The selection of the most suitable model depends on the fitting accuracy and on the deformation interval in which the material response is stable. The stability criterion evaluates whether the deformation energy is positive. When a material model is unstable and a component deforms through that instability, the result is non-physical behavior that can cause nonconvergence. Since the stress-strain response of hyperelastic materials is loading mode dependent, there is important to minimize model fit errors in that loading mode that is predominant. For this reason, the visual evaluation of the user is as important as the mentioned criteria. Based on the presented results, it can be stated that the best fitting and stable model was provided by Marlow form.

Acknowledgement

This work was supported by the grant project VEGA 1/0355/18 funded by Vedecká grantová agentúra MŠVVaŠ SR and SAV.

References

[1] M.F. Beatty, D.O. Stalnaker, The Poisson function of finite elasticity, Journal of Applied Mechanics (1986), 807–813, https://www.researchgate.net/publication/245358311_The_Poisson_Function_of_Finite_Elasticity.

[2] B. Sanborn, B. Song, Poisson's Ratio of Hyperelastic Foam Under Quasi-Static and Dynamic Loading, International Journal of Impact Engineering (2019) 48–55, ISSN 0734-743X.

[3] Abaqus documentation, retrieved from: https://abaqus-docs.mit.edu/2017/English/SIMACAEMATRefMap/simamat-c-hyperelastic.htm.

[4] STN ISO 37: Rubber, vulcanized or thermoplastic. Determination of tensile stress-strain properties (in Slovak), 2008.

[5] M. Hagara, R. Huňady, F. Trebuňa, Stress Analysis Performed in the Near Surrounding of Small Hole by a Digital Image Correlation Method, In: Acta Mechanica Slovaca 18 (3-4), 2014, p. 74–81.